InGaN channel high electron mobility transistor structures grown by metal organic chemical vapor deposition

O. Laboutin,[1] Y. Cao,[1] W. Johnson,[1] R. Wang,[2] G. Li,[2] D. Jena,[2] and H. Xing[2]
[1]*Kopin Corporation, 200 John Hancock Road, Taunton, Massachusetts 02780, USA*
[2]*Department of Electrical Engineering, University of Notre Dame, Notre Dame, Indiana 46556, USA*

(Received 9 February 2012; accepted 7 March 2012; published online 23 March 2012)

High electron mobility transistor (HEMT) structures of AlInGaN/AlN/InGaN/GaN were grown by metal-organic chemical vapor deposition. A combination of low growth rate and high growth temperature during synthesis of the InGaN channel layer led to significant improvement in HEMT electron transport properties. The improvement was correlated with an evolution of both surface roughness and photoluminescence intensity of InGaN. Record electron mobilities from 1070 to 1290 $cm^2/V{\cdot}s$ with associated sheet charge density of $\sim 2 \times 10^{13}\,cm^{-2}$ were obtained across the $In_xGa_{1-x}N$ channel composition range $x = 0.05$ to 0.10. © *2012 American Institute of Physics*. [http://dx.doi.org/10.1063/1.3697415]

While GaN-based high electron mobility transistors (HEMTs) have demonstrated record DC and RF power performance attributable to underlying material properties, some physical limitations exist when scaling conventional GaN HEMTs to deep submicron dimensions required for ultra-high frequency operation. To mitigate short-channel effects and ensure adequate pinchoff characteristics at high drain bias, it is necessary to appropriately scale the L_g/t_{bar} ratio, where L_g is device gate length and t_{bar} is the thickness of the wide bandgap barrier layer under the gate.[1] For conventional AlGaN/GaN HEMTs, the two-dimensional electron gas (2DEG) density rapidly decreases with decreasing t_{bar}, resulting in a minimum practical barrier thickness of 10–15 nm, thus limiting minimum gate length and peak operation frequency. Owing to significantly larger spontaneous polarization charge, AlInN-based HEMTs with barrier thickness of only 6–10 nm have demonstrated marked improvements in drain current[2] and cutoff frequency[3,4] relative to conventional AlGaN/GaN HEMTs. However, since the 2DEG in AlInN/GaN HEMT structures is formed in the GaN channel without 2DEG confinement from the buffer side, such devices still suffer from short-channel effects.[3,5] To address this limitation and spatially confine channel electrons, two back-barrier concepts have been proposed for GaN-based HEMTs: an AlGaN buffer layer[6] and a thin InGaN polarization barrier between GaN buffer and GaN channel layers.[7] However, the AlGaN buffer approach suffers from poor AlGaN material quality and low buffer thermal conductivity. For the InGaN back-barrier HEMT, material quality of the GaN channel can be degraded due to InGaN roughness. Furthermore, electrons from the 2DEG may be injected into the back-barrier under high drain bias, potentially leading to screening of the piezoelectric field in the back-barrier and degradation of electron confinement.

The most robust and straightforward solution to this problem would be a narrow bandgap channel layer formed between the wide bandgap barrier and the GaN buffer, similar to the approach widely used in GaAs pHEMTs. Recently, there have been several attempts to employ InGaN as a channel in AlGaN-based and InAlN-based HEMTs.[8–12] In these structures, the GaN buffer layer below the InGaN channel served as a natural back-barrier and improved electron confinement as verified by capacitance-voltage measurements.[8,11] However, all the HEMT structures with InGaN channel synthesized so far exhibited high sheet resistance due to either low mobility or low carrier density. It has been suggested that both interface roughness (IR) scattering and alloy scattering in the InGaN channel are responsible for these reduced transport properties.[12] Further compounding the problem, although AlInN-based HEMTs are advantageous for L_g/t_{bar} scaling, the strong polarization field in these structures pushes the 2DEG centroid closer to the barrier than in AlGaN-based structures and thus elevates IR scattering.[13] In this work, we demonstrate enhancement of electron mobility in InGaN channel HEMTs by reduction of both IR and alloy scattering. Through the optimization of metal organic chemical vapor deposition (MOCVD) conditions, record transport properties for HEMTs employing an InGaN channel are obtained.

All growths were performed in a close-coupled showerhead MOCVD reactor operating at low pressure. The nominally undoped AlInGaN/AlN/InGaN/GaN HEMT structures of this study consisted of thin GaN or AlN nucleation layer, 1.9 μm thick GaN back-barrier buffer layer, 5–9 nm thick $In_xGa_{1-x}N$ channel, 11 nm thick composite AlInGaN/AlN barrier and were grown on sapphire substrates unless otherwise noted. Optimization of the composite barrier consisting of quaternary AlInGaN near lattice-matched to GaN and AlN spacer has been described elsewhere.[14] Growth temperature was about 750 °C for the barrier layer and varied in the range of 710–790 °C for the InGaN channel layer as verified by pyrometer measurements. Growth rate and composition of the InGaN channel were controlled by adjusting trimethyl gallium (TMG) and trimethyl indium (TMI) molar fluxes, respectively. In order to grow an InGaN channel with fixed InN molar fraction of 0.06, the TMI flux was increased from 1.5 to 25 μmol/min when the growth temperature increased from 710 to 790 °C. The TMG flux was decreased from 18 to 6 μmol/min decreasing growth rate of InGaN from 0.03 to 0.08 nm/s. The thickness and composition of the InGaN

channel were calibrated using thick single InGaN layers and InGaN/GaN multilayer structures characterized by high resolution x-ray diffraction and room temperature photoluminescence (PL). The InGaN composition in thin layers was verified using PL. Thickness of the AlInGaN/AlN barrier was estimated using x-ray reflectivity. Electron transport properties were studied by room temperature Hall-effect measurements and sheet resistance (R_{sh}) was mapped using contactless eddy current measurements.

The 6 nm thick InGaN channel in AlInGaN/AlN/InGaN/GaN HEMT structures was initially grown at 750 °C employing 0.08 nm/s growth rate. Measured HEMT 2DEG sheet charge density was $\sim 2 \times 10^{13}$ cm^{-2} with only a weak dependence on In content of the $In_xGa_{1-x}N$ channel. However, when In content increased from $x = 0.02$ to $x = 0.10$, the 2DEG mobility decreased from 690 to 260 cm^2/V·s. Due to lattice mismatch, the InGaN channel is compressively strained by the underlying GaN buffer and can form a rough surface before the AlN spacer is grown on top. Alloy scattering, the other factor believed to limit mobility, is caused by randomly varying alloy potential in the channel and is intrinsic at the atomic scale. However, indium segregation phenomena are well-known in InGaN films and such segregation can change electron effective mass and electron potential energy, resulting in alloy scattering at the mesoscopic scale.

In order to estimate the roughness of the channel-barrier interface, we interrupted growth after the InGaN and checked the surface morphology using atomic force microscopy (AFM). The AFM surface topography of 9 nm thick $In_{0.06}Ga_{0.94}N$ layer grown with 0.08 nm/s growth rate at 710 °C revealed significant roughness (RMS $\Delta \sim 0.8$ nm) due to surface pits and trenches as seen in Fig. 1(a). The cross sectional analysis of the AFM surface topography further revealed the average distance between surface trenches of about 160 nm and average trench/pit depth of about 2.6 nm. In attempt to smooth the InGaN surface, both lower growth rate and higher growth temperature were explored during synthesis of uncapped InGaN samples. Fig. 1(b) shows the AFM surface topography of a 9 nm thick $In_{0.06}Ga_{0.94}N$ layer grown with 0.03 nm/s growth rate at 790 °C, clearly illustrating improvement in the surface morphology. RMS reduced to $\Delta \sim 0.5$ nm while the average distance between surface trenches increased to about 260 nm and average trench/pit depth decreased to about 1.2 nm. Similar trend of decreasing InGaN surface roughness with decreasing growth rate and increasing growth temperature was observed on SiC substrate. In the IR scattering model, IR-limited electron mobility is proportional to $1/\Delta^2$. Therefore, an obvious improvement in mobility is expected from reduced surface roughness of InGaN.

Interestingly, the improvement of the InGaN surface roughness was accompanied by a significant change in the room temperature PL intensity. Two HEMT samples with 5 nm thick $In_{0.08}Ga_{0.92}N$ channel grown under two different sets of growth conditions, one with 0.08 nm/s growth rate at 750 °C and the other with 0.03 nm/s growth rate at 790 °C were studied by PL measurements. The PL spectra from this study are reported in Figure 2. The main PL peak originated from the InGaN channel and was centered near 3 eV for both samples. Other peaks centered near 3.4 and 2.2 eV were associated with the near band-edge and yellow band emissions from GaN. The intensity of the main peak was strikingly different, more than two orders of magnitude lower in the sample grown with low growth rate and at high temperature. High luminescence efficiency in InGaN alloys is often ascribed to a localization of free carriers at centers associated with composition and/or thickness fluctuations.[15,16] Thus, it can be inferred that the reduced PL intensity of the InGaN channel grown with low growth rate and at high growth temperature is an indicator of improved composition and/or thickness uniformity compared to the sample grown with high growth rate and at low temperature. This was verified by Hall effect measurements where electron mobility of a HEMT with 5 nm $In_{0.08}Ga_{0.92}N$ channel increased dramatically from 350 to 1050 cm^2/V·s when both low growth rate of 0.03 nm/s and high growth temperature of 790 °C were introduced for deposition of the InGaN channel.

To further demonstrate the improvement in transport properties by the combination of low growth rate and high growth temperature for the InGaN channel, a series of AlInGaN/AlN/InGaN/GaN HEMT structures with varying InGaN channel composition were grown on SiC substrates. For these structures, thickness of the InGaN channel was held constant at 5 nm. An AlInGaN/AlN/GaN structure with conventional GaN channel was grown as a reference. The 2DEG sheet charge density was again constant at $\sim 2 \times 10^{13}$ cm^{-2} for all InGaN channels. Fig. 3(a) shows electron mobility as a function of InGaN channel composition as well as previously reported HEMT mobility values from the literature. In our study, the electron mobility monotonically decreased from 1690 cm^2/V·s in the GaN channel to 1070 cm^2/V·s in the $In_{0.1}Ga_{0.9}N$ channel. The trend of decreasing electron mobility with increasing In concentration seen in Fig. 3(a) is

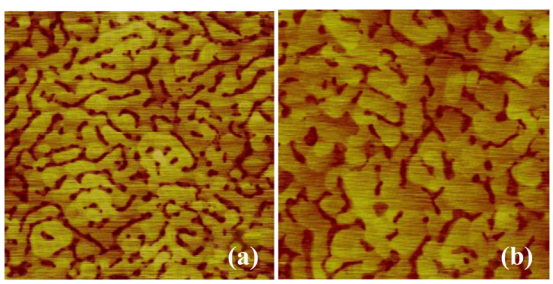

FIG. 1. 2 μm × 2 μm AFM images of 9 nm uncapped $In_{0.06}Ga_{0.94}N$ grown (a) with 0.08 nm/s growth rate at 710 °C and (b) with 0.03 nm/s growth rate at 790 °C. Height contrast of AFM images is 5 nm.

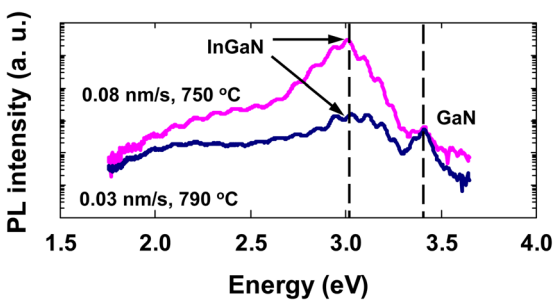

FIG. 2. Room temperature photoluminescence spectra of two AlInGaN/AlN/InGaN/GaN HEMTs with 5 nm $In_{0.08}Ga_{0.92}N$ channel grown with 0.08 nm/s growth rate at 750 °C and with 0.03 nm/s growth rate at 790 °C.

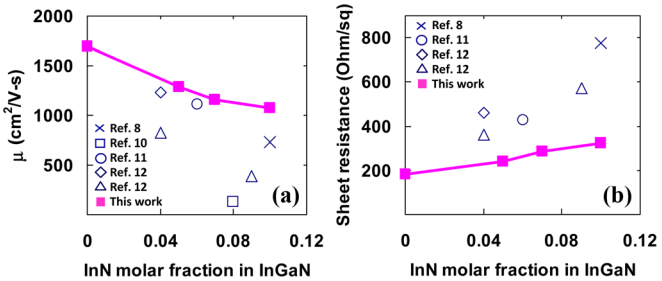

FIG. 3. Electron mobility as a function $In_xGa_{1-x}N$ channel composition for HEMT structures of this work (■) and from the literature. Other data include Ref. 8 (×) for $Al_{0.25}Ga_{0.75}N$ barrier and $n_s = 1.1 \times 10^{13}\,cm^{-2}$, Ref. 10 (□) for $Al_{0.33}Ga_{0.67}N$ barrier and $n_s = 1.5 \times 10^{13}\,cm^{-2}$, Ref. 11 (**O**) for $Al_{0.3}Ga_{0.7}N$ barrier and $n_s = 1.3 \times 10^{13}\,cm^{-2}$, Ref. 12 (◇) for $Al_{0.24}In_{0.01}Ga_{0.75}N$ barrier and $n_s = 1.1 \times 10^{13}\,cm^{-2}$, and Ref. 12 (Δ) for $Al_{0.83}In_{0.17}N$ barrier and $n_s = 2.1 - 2.8 \times 10^{13}\,cm^{-2}$.

similar to observations from AlGaN-based structures.[10,11] A record high electron mobility of 1290 $cm^2/V{\cdot}s$ was obtained for the HEMT structure with InN molar fraction of 0.05. In spite of higher sheet charge density in our structures, the electron mobility was higher than that in the AlGaN structures[8,9,11] within the entire $In_xGa_{1-x}N$ compositional range $0 \le x \le 0.1$. The results achieved in this work also exceeded the mobility reported for HEMT structures with $Al_{1-y}In_yN$/AlN ($y = 0.16 - 0.2$) and $Al_{0.24}In_{0.01}Ga_{0.75}N$/AlN barriers with $In_xGa_{1-x}N$ ($x = 0.04 - 0.09$) channel.[12] The superior transport properties of AlGaInN/AlN/GaInN/GaN HEMT structures from this study are illustrated in Fig. 3(b) reporting the sheet resistance versus InGaN channel composition. Sheet resistance mapping across a 3 in wafer with $In_{0.05}Ga_{0.95}N$ channel produced an average value of 240 Ω/sq with standard deviation of 4.2%.

In conclusion, by optimizing growth conditions for InGaN, we have demonstrated a record high electron mobility window of 1070–1290 $cm^2/V{\cdot}s$ for AlInGaN/AlN/InGaN/GaN HEMT structures with $In_xGa_{1-x}N$ ($x = 0.05 - 0.10$) channel. This study provides an approach to obtain high quality back-barrier HEMTs with improved carrier confinement for advanced high power and high speed device applications.

The work at Kopin Corporation was partially supported by the Missile Defense Agency (MDA) via SBIR funding (Contract No. W9113M-10-C-0066) monitored by John Blevins. The authors (O.L., Y.C., and W.J.) also acknowledge the ongoing support of Daily Hill, Hong Choi and the III-V Product Group at Kopin Corporation.

[1]G. H. Jessen, R. C. Fitch, J. K. Gillespie, G. Via, A. Crespo, D. Langley, D. J. Denninghoff, M. Trejo, and E. R. Heller, IEEE Trans. Electron Devices **54**, 2589 (2007).
[2]H. Wang, J. W. Chung, X. Gao, S. Guo, and T. Palacios, Phys. Status Solidi C **7**, 2440 (2010).
[3]D. S. Lee, X. Gao, S. Guo, D. Kopp, P. Fey, and T. Palacios, IEEE Electron Device Lett. **32**, 1525 (2011).
[4]R. Wang, G. Li, J. Verma, B. Sensale-Rodriguez, T. Fang, J. Guo, Z. Hu, O. Laboutin, Y. Cao, W. Johnson, G. Snider, P. Fay, D. Jena, and H. Xing, IEEE Electron Device Lett. **32**, 1215 (2011).
[5]J. Song, F. J. Xu, X. D. Yan, F. Lin, C. C. Huang, L. P. You, T. J. Yu, X. Q. Wang, B. Shen, K. Wei, and X. Y. Liu, Appl. Phys. Lett. **97**, 232106 (2010).
[6]D. S. Lee, X. Gao, S. Guo, and T. Palacios, IEEE Electron Device Lett. **32**, 617 (2011).
[7]J. Liu, Y. Zhu, K. M. Lau, and K. J. Chen, IEEE Electron Device Lett. **27**, 10 (2006).
[8]G. Simin, X. Hu, A. Tarakji, J. Zhang, A. Koudymov, S. Saygi, J. Yang, A. Khan, M. S. Shur, and R. Gaska, Jpn. Appl. Phys. **40**, L1142 (2001).
[9]G. Simin, A. Koudymov, H. Fatima, J. Zhang, J. Yang, A. Khan, X. Hu, A. Tarakji, R. Gaska, and S. Shur, IEEE Electron Device Lett. **23**, 458 (2002).
[10]H. Ikki, Y. Isobe, D. Iida, M. Iwaya, T. Takeuchi, S. Kamiyama, I. Akasaki, H. Amano, A. Bandoh, and T. Udagawa, Phys. Status Solidi A **208**, 1614 (2011).
[11]N. Okamoto, K. Hoshino, N. Hara, M. Takikawa, and Y. Arakawa, J. Cryst. Growth **272**, 278 (2004).
[12]J. Xie, J. H. Leach, X. Ni, M. Wu, R. Shimada, U. Ozgur, and H. Morkoc, Appl. Phys. Lett. **91**, 262102 (2007).
[13]Y. Cao and D. Jena, Appl. Phys. Lett. **90**, 182112 (2007)
[14]O. Laboutin, Y. Cao, R. Wang, G. Li, D. Jena, H. Xing, C.-F. Lo, L. Liu, S. J. Pearton, F. Ren, and W. Johnson, ECS Trans. **41**(8), 301 (2011), edited by K. Shenai, M. Dudley, R. Garg, A. Khan, and R. Ma.
[15]Y. Narukawa, Y. Kawakami, M. Funato, S. Fujita, S. Fujita, and S. Nakamura, Appl. Phys. Lett. **70**, 981 (1997).
[16]J. Narayan, H. Wang, J. Ye, S.-J. Hon, K. Fox, J. C. Chen, H. K. Choi, and J. C. C. Fan, Appl. Phys. Lett. **81**, 841 (2002).